Veterinary
Anaesthesia and Analgesia
Formerly the Journal of Veterinary Anaesthesia

Veterinary Anaesthesia and Analgesia, 2014 doi:10.1111/vaa.12224

RESEARCH PAPER

Comparison of three ultrasound guided approaches to the lumbar plexus in dogs: a cadaveric study

Sophie M Graff*, Deborah V Wilson†, Laurent P Guiot‡ & Nathan C Nelson*

*Department of Small Animal Clinical Sciences, College of Veterinary Medicine, Michigan State University, East Lansing, MI, USA

†Department of Large Animal Clinical Sciences, College of Veterinary Medicine, Michigan State University, East Lansing, MI, USA

‡Department of Veterinary Clinical Sciences, College of Veterinary Medicine, The Ohio State University, Dublin, OH, USA

Correspondence: Laurent P Guiot, Department of Veterinary Clinical Sciences, College of Veterinary Medicine, The Ohio State University, 5020 Bradenton Avenue, Dublin, OH 43017, USA. E-mail: guiotlau@gmail.com

Abstract

Objective To assess the accuracy of contrast material injection and the dispersion of injectate following ultrasound guided injections at the level of L6 and L7, in canine cadavers.

Study design Prospective, randomized, experimental study.

Animals Twenty nine mixed breed canine cadavers (28.9 ± 6.0 kg).

Methods Three ultrasound-guided approaches to the lumbar plexus (LP) were compared: 1) a dorsal pre-iliac approach at the level of L6; 2) a lateral paravertebral approach at mid-L6; and 3) a lateral paravertebral approach at mid-L7. An isovolumic mixture of iodine-based contrast with new methylene blue (0.1 mL kg^{-1}) was injected bilaterally in the juxta-foraminal region along the L6 or L7 nerve root. Computed tomography was performed followed by segmentation and 3D reconstruction of the lumbar spine and contrast material volumes using dedicated software. Distances between contrast material and the fifth through seventh lumbar foraminae, and length of femoral (FN) and obturator (ON) nerve staining were measured and compared between approaches ($p < 0.05$).

Results Injectate moved cranial and caudal to the site of injection, and dispersed into an ovoid shape between the quadratus lumborum, iliopsoas and psoas minor muscles. Injections at L7 resulted in significantly closer contrast proximity to the L6 and L7 foraminae ($p < 0.001$). Femoral nerve staining was similar for all approaches, ON staining was more consistent after L7 injections ($p < 0.001$).

Conclusion and clinical relevance An ultrasound-guided lateral paravertebral approach to the LP proved very practical and accurate, with easy visualization of the plexus and associated nerves. To ensure that the ON is covered by injectate, an approach at the level of L7 is recommended. Further studies are necessary to determine if this correlates with clinically effective local anesthesia.

Keywords canine, local anesthesia, nerve block, ultrasound.

Introduction

Regional anesthetic techniques such as peripheral nerve blocks are gaining popularity to provide both intraoperative antinociception and postoperative analgesia in dogs undergoing pelvic limb surgery (Portela et al. 2010, 2012; Campoy et al. 2012; Caniglia et al. 2012; Vettorato et al. 2012). They have an increased selectivity compared to neuraxial

(epidural) blockade and have the potential for providing reliable analgesia with low complication rates, thus improving anesthetic safety (Vettorato et al. 2012). Furthermore, meta-analysis of clinical trials comparing regional anesthetic techniques in people show equivalence in terms of efficacy and improved safety profiles of peripheral techniques compared to epidural (Fowler et al. 2008). In dogs, peripheral nerve blocks could result in avoidance of known epidural-related complications such as hypotension, urinary retention and alopecia (Hendrix et al. 1996; Jones 2001).

Pelvic limb nerve blockade entails a combination of a cranial injection centered over the lumbar plexus (LP) or over the femoral nerve (FN) and a caudal injection over the sciatic nerve (ScN). While the choice of ScN injection site and technique causes little debate, several approaches using various landmarks and techniques have been devised for the cranial component of pelvic limb nerve blockade in dogs (Campoy et al. 2008; Echeverry et al. 2010; Caniglia et al. 2012). Nerve stimulation is commonly used in conjunction with anatomical landmark palpation to guide the injection prior to peripheral nerve block (Mahler & Adogwa 2008; Portela et al. 2010, 2012; Campoy et al. 2012; Caniglia et al. 2012; Vettorato et al. 2012). Despite the potential for aiding in nerve localization, nerve stimulation does not guarantee injection accuracy. Injection away from or within nerve fascicles may occur with nerve stimulation and result in peripheral nerve block failure or iatrogenic nerve injuries, respectively (Rasmussen et al. 2006; Campoy et al. 2008; Jeng & Rosenblatt 2011; Caniglia et al. 2012; Vettorato et al. 2012). Real-time visualization of targeted nerves during injection has the potential to circumvent these limitations and can be achieved through ultrasound imaging.

Ultrasonographic (U/S) guidance for regional anesthesia offers several advantages, including direct visualization of the target nerves, the needle, and the spread of local anesthetic solution during injection. This technique may reduce the need for multiple needle passes, thus reducing potential tissue damage, and allow repositioning in case of suboptimal local anesthetic distribution (Marhofer et al. 2005). Overall, the use of ultrasound has improved the safety and quality of nerve blockade in people (Enneking et al. 2005).

Success of peripheral nerve blockade is contingent upon local anesthetic delivery to all sensory branches coming from a surgical site. While the research focus of pelvic nerve block techniques has been centered on FN blockade (Echeverry et al. 2012a,b; Mahler 2012), pelvic limb sensory innervation also includes the obturator (ON), lateral femoral cutaneous and ScN (Adams 2004; Evans & de Lahunta 2013). More specifically, stifle sensory innervation includes branches of the medial articular nerve which contains branches of the ON in up to 50% of dogs (O'Connor & Woodbury 1982). It has been proposed that an unblocked ON in humans could account for some cases of patchy anesthesia or failure of the block (Sakura et al. 2010) and improved surgical analgesia is achieved when specific ON blockade is added to FN and ScN blocks (McNamee et al. 2002; Macalou et al. 2004; Sakura et al. 2010). The anatomical evidence (O'Connor & Woodbury 1982) suggests that the ON is also relevant for dogs undergoing surgery of the stifle. The FN and ON are contiguous proximally and their continuity with the LP might allow capture of both by a single injection.

Therefore, the purpose of this study was to develop a practical, accurate and repeatable ultrasound-guided paravertebral approach to the LP targeting the FN and ON. The objectives were to assess the accuracy of U/S-guided injections and dispersion of injectate following three approaches to the LP, using computed tomography (CT) imaging, and to determine the degree of FN and ON staining following each approach, in canine cadavers. First, a pilot study was performed aimed at mapping the FN, ON and ScN topography in the lumbosacral region using nerve enhancement and CT of the lumbar spine and pelvis, with 3-dimensional (3-D) reconstruction of the area. It was hypothesized that at the sixth lumbar vertebra (L6) either a dorsal pre-iliac or a lateral paravertebral approach with U/S guidance would be equally effective for FN imaging and staining. A second hypothesis, derived after evaluation of the pilot study results, was that a more caudal approach to the LP at the level of L7 would provide better capture of the ON as compared to either approach at L6.

Materials and methods

The study was approved by the Institutional Animal Care and Use Committee, and Clinical Research Committee. All dogs were euthanized for reasons unrelated to this research project and frozen immediately after euthanasia. The cadavers were thawed for 2 days before the study, clipped and washed the

morning of the procedures. The research included three parts: 1) a pilot study was first performed to evaluate the U/S appearance and CT scan topographic relationship of the FN and ON with respect to the sublumbar musculature and lumbosacral spine; 2) two U/S guided approaches at the level of L6 were compared using similar landmarks previously described for use with nerve stimulation; and 3) an approach at the level of L7 was developed in order to capture the ON, and this was compared to the L6 approaches.

Pilot study

In one canine cadaver, the FN, ON and ScN were enhanced for U/S and CT detection. After surgically isolating each nerve distal to the stifle, a 0.89 mm intravascular wire (Weasel Wire; Infiniti Medical LLC, CA, USA) was threaded within the epineurium of each nerve. The wires were advanced manually up to the spinal cord under CT guidance. The lumbar plexus was then evaluated ultrasonographically and an injection of contrast solution was made near the L6 foramen. Finally, CT imaging and segmentation were performed. The relationships between the FN, ON, contrast material and the surrounding structures were evaluated and recorded.

Study protocols

Study 1

A comparison of the dorsal pre-iliac and the lateral paravertebral approaches at L6 was performed. Nineteen mixed breed canine cadavers, average weight (±SD) 21.5 ± 6.0 kg were studied.

An approach to both left and right LP at L6 was made, using either the dorsal pre-iliac or the lateral paravertebral approach. For each side the approach was randomized prior to the study, using the Excel random number generator. All data including CT analysis and dissection evaluation were compared between approaches.

Study 2

An evaluation of the feasibility and accuracy of the lateral paravertebral approach to the FN and ON, when performed one vertebral body more caudal at the mid-body of L7, was subsequently performed using another ten mixed breed canine cadavers, average weight (±SD) 28.9 ± 6.5 kg. Two ultrasound-guided approaches to the LP and subsequent injections (left and right sides at L7) were performed in each cadaver. All data from CT analysis and dissection were compared to those previously collected in study 1.

Injection and imaging techniques

Ultrasound imaging and contrast injections were performed with the dogs in lateral recumbency, selected lumbar plexus uppermost, with pelvic limbs in a neutral position. In each dog, the paralumbar area was imaged with a variable frequency linear U/S transducer (GE Logiq P5; GE Healthcare, NJ, USA). The highest U/S frequency that allowed visualization of the lumbar vertebral bodies was used, typically 7 MHz in larger dogs and 10 MHz in smaller dogs. If vertebral body depth was too great (one dog), a microconvex variable frequency transducer was used at an imaging frequency of 8 MHz. All injections consisted of a total volume of 0.1 mL kg^{-1} of an isovolumic mixture of iodine based contrast (ISOVUE-300 Iopamidol injection 61%; Bracco Diagnostics Inc., NJ, USA by Patheon Italia S.p.A, Italy) and new methylene blue (NMB; Akron, Inc., IL, USA).

Immediately following the injections, dogs were positioned in dorsal recumbency within a trough for CT scan imaging with their pelvic limbs semi-extended in a frog legged position. Transverse CT images were acquired from the cranial lumbar area through the pelvic outlet (GE Brightspeed; GE Healthcare). The following acquisition parameters were used: 1.25 mm slice thickness, collimator pitch 1.0, mA 250, kVp 120, standard reconstruction algorithm. An evaluator, blinded to the approach, recorded measurements based on cross-sectional images including contrast length, location with respect to the lumbar and sacral vertebrae, and distance of the contrast from a fixed bony landmark at the foramen of L5-6, L6-7 and L7-S1. Dimensions were normalized by indexing them to the length of the vertebral body of L6. Where a filling defect was observed, the length was measured by evaluating serial slices from beginning to end of the observed defect. The presence of any contrast agent in the abdominal cavity or epidural space was noted. Tomographic images were then imported into a specialized CT analysis software package (Mimics 14.0; Materialise, Belgium). This program was used to create 3-D images following segmentation of the original images. A 3-D sculpting tool was used on

the 3-D model to isolate the injectate. Small portions of muscle in contact with the contrast were removed manually, slice-by-slice, from the mask using a two-dimensional editing tool. Contrast volume shape and topography were recorded.

Following the CT imaging, an evaluator, blinded to the approach, dissected the lumbar plexus (L4 to L7) utilizing a lateral approach. A lateral paralumbar skin incision was made and continued in the subcutaneous tissues to expose the ventral aspect of the epaxial musculature from the level of L3 to the ilial body. Once the iliopsoas muscle was elevated ventrally from its origin on the 4th through 7th lumbar vertebral transverse processes, and from the corresponding vertebral bodies, the cranial aspect of the lumbar plexus, including the L4–L7 nerve roots, along with the FN and ON were seen. A digital image, including a calibration marker, was obtained following each dissection. The FN and ON were recorded as stained (positive) where length of staining was ≥2 cm. This length was chosen to reflect the estimated length of nerve exposure to local anesthetic required to block impulse transmission (Raymond et al. 1989; Campoy et al. 2008).

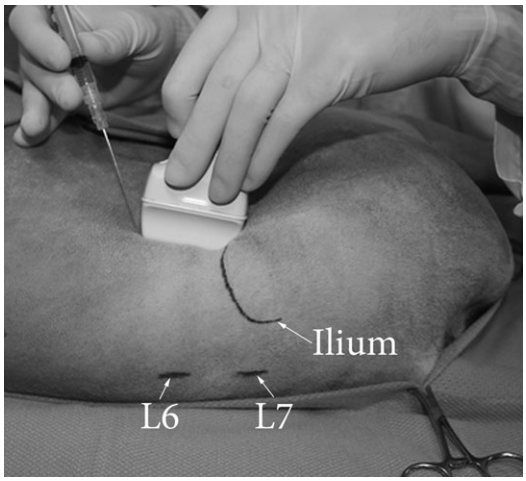

Figure 1 Ultrasound probe position and anatomical landmarks in a dog used for the lateral paravertebral approach to the lumbar plexus at mid-L6 (approach at mid-L7 appears similar). The dog is in lateral recumbency, cranial is to the left. L6, L7 are spinous processes of the 6th and 7th lumbar vertebrae.

Description of approaches

Three U/S-guided approaches to the LP were derived for this study. The first two approaches used in Study 1 were centered over L6 while the third approach was centered more caudally, at the level of L7.

Lateral paravertebral approach at L6

First, the transducer was placed in a dorsal plane to image the wing of the ilium (Fig. 1) The probe was then advanced cranially, and the most lateral aspect of L7 transverse process was identified. The transducer was advanced further cranially, and the lateral aspect of L6 vertebral transverse process was identified. The transducer was then moved ventrally and medially until the ventrolateral aspect of the L6 vertebral body was identified. By then angling the ultrasound beam slightly dorsally, a large nerve root exiting the L5–6 intervertebral foramen was seen. Maintaining the U/S transducer in this position, a 22 gauge 63 mm spinal needle (BD Spinal Needle; BD Medical, NJ, USA) was advanced in plane from the cranial aspect of the transducer, until the tip of the needle was immediately adjacent to (but not contacting) the LP at the level of the mid-vertebral body. The injection of contrast solution was then directly observed.

Dorsal pre-iliac approach at L6

The transverse process of L6 was identified similarly to the previous approach. This transverse process was then followed medially to the dorsal aspect of the L6 vertebral body. The transducer was then rotated into a transverse plane, and moved just caudal to the L6 transverse process (Fig. 2) This provided a transverse image approximately at the level of mid-body L6. A large nerve (arising from L5–6 intervertebral foramen) could then be seen in cross-section, adjacent to the vertebral body. Maintaining the transducer in a transverse plane, a 22 gauge 63 mm spinal needle (BD Spinal Needle; BD Medical) was advanced in plane from the dorsal aspect of the transducer, so that the tip of the needle was immediately adjacent to the large nerve root. The injection of contrast was then directly observed.

Lateral paravertebral approach at L7

A dorsal pre-iliac approach at L7 was not feasible, but a lateral approach was possible. Following identification of the L6–7 intervertebral disc, using the same probe position as for the L6 approach, the U/S transducer was fanned to direct the U/S beam more dorsally until the nerve root exiting the L6–7

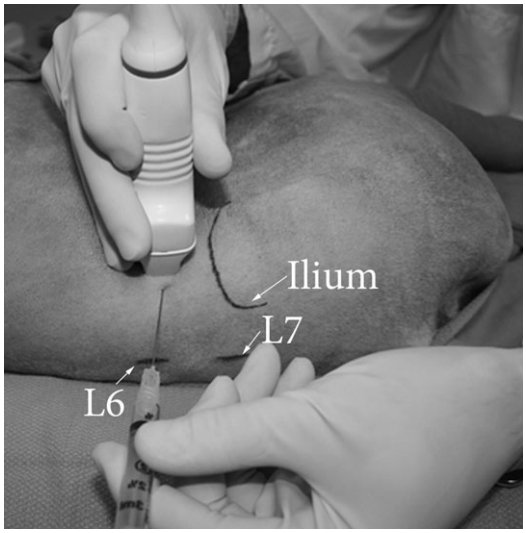

Figure 2 Ultrasound probe position and anatomical landmarks in a dog using the dorsal pre-iliac approach to the LP. The dog is in lateral recumbency, cranial is to the left. L6, L7 are spinous processes of the 6th and 7th lumbar vertebrae.

intervertebral foramen was seen. The probe was manipulated to place this nerve in long axis. Maintaining this plane, a 22 gauge 63 mm spinal needle (BD Spinal Needle; BD Medical) was advanced in plane from the cranial aspect of the transducer, so that the tip of the needle was immediately adjacent to the large nerve root near the level of mid-L7. The injection of contrast was then directly observed.

Statistical analysis

All parametric data are presented as mean ± SD, and were analyzed using ANOVA (SigmaPlot 11.0; Systat software, Inc., CA, USA) Length of contrast measured was normalized by indexing to the length of the vertebral body of L6. When there were significant ($p < 0.05$) main effects, means were compared using all pairwise multiple comparison procedures (Dunn's method). Where Normality testing failed, ANOVA was performed on ranks. Categorical data were compared using Fishers exact test (http://vassarstats.net; accessed February, 2014).

Results

Pilot study

Three-dimensional reconstruction of the lumbar spine allowed examination of the relationship between FN, ON and ScN and the adjacent bony structures (Fig. 3a & b). The epineural wires also allowed us to confirm the sonographic appearance and the topographic localization of the FN (Figs 4 & 5). The FN as it merges with the LP was seen in close proximity to the lumbar vertebral bodies on each side of the spine (Fig. 5), with individual nerves diverging separately between the muscle bellies of the iliopsoas and psoas minor. The relationship of the contrast depot to the LP was visible, as was the

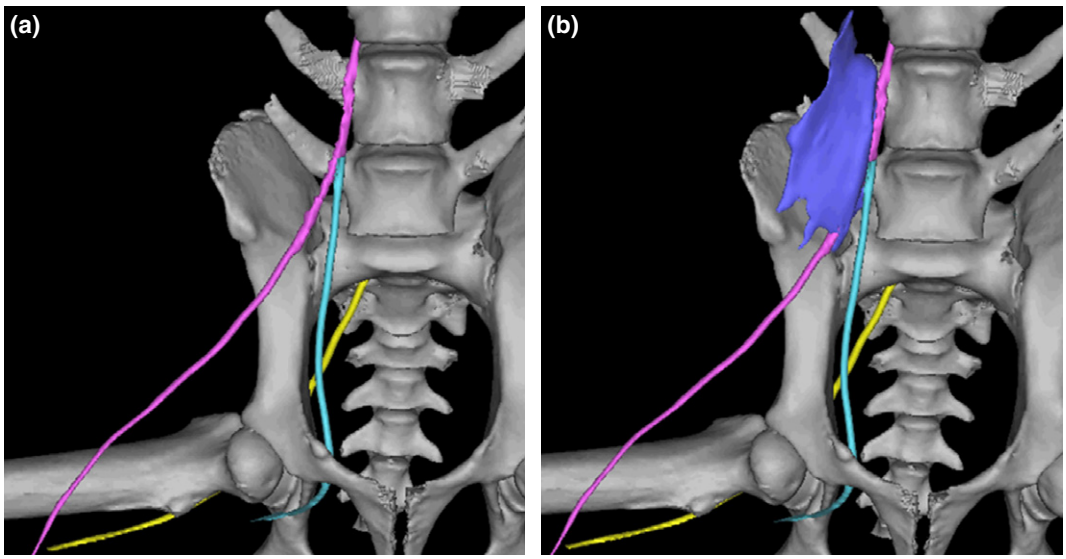

Figure 3 (a, b) Ventral view of a three-dimensional reconstruction from tomographic images of lumbar spine and pelvis in a dog prior to and following injection of contrast utilizing a lateral paravertebral injection at L6. Three nerves were highlighted by radiopaque guide wires threaded within the epineurium, and here are depicted in colors: obturator (turquoise), femoral (pink) and sciatic (yellow). In (b), contrast agent is colored purple.

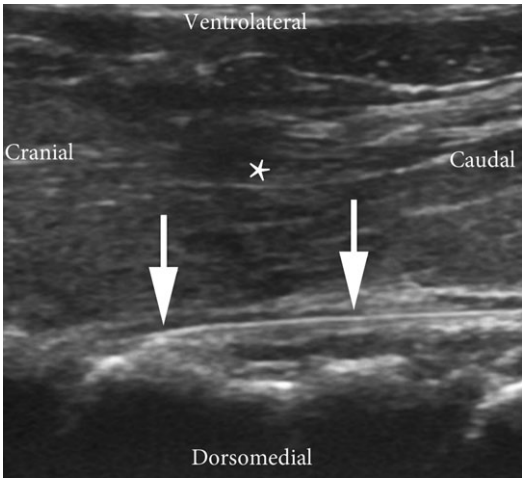

Figure 4 Ultrasound image of the femoral nerve (FN) component of the lumbar plexus (LP) after epineural insertion of an hydrophilic wire in a dog using the lateral paravertebral approach to the LP at mid-L6. A longitudinal image of the FN is evident as a linear hypoechoic structure (white arrows). The LP at that level is enclosed in fascia within the muscle bellies of the iliopsoas muscle (*).

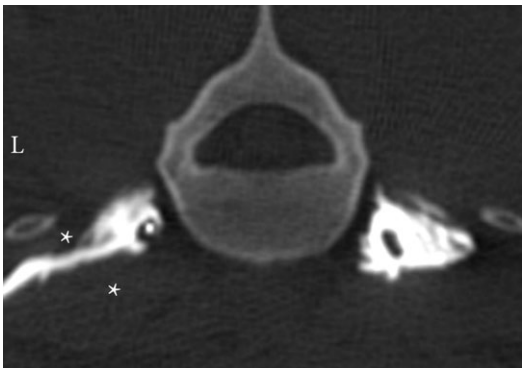

Figure 5 Tomographic images of the mid-L6 area following lateral paravertebral (left) and dorsal pre-iliac (right) contrast injection adjacent to the LP under ultrasound guidance. A filling defect is clearly imaged within the contrast on both sides. The radiopaque wire can be seen within the filling defect on the left side. The LP, at that level, is enclosed in fascia within the muscle bellies of the iliopsoas muscle (*).

filling defect created by the FN and ON components of the LP within that contrast (Fig. 6a & b).

Study protocols

Study 1 – comparison of the dorsal and lateral approaches at L6

Both approaches (the dorsal and lateral) at L6 allowed imaging of the nerves of the LP, the needle

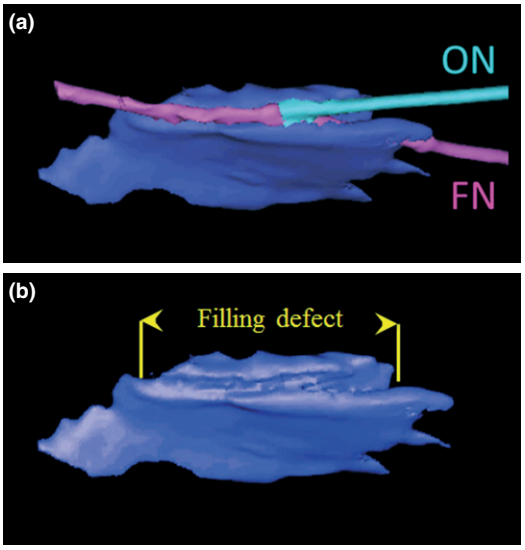

Figure 6 (a, b) Three-dimensional reconstruction from tomographic images of the contrast volume after select nerves were highlighted with guide wires. Relationship between the contrast agent (purple) and the femoral nerve (FN, pink) and obturator nerve (ON, turquoise). In (b), a filling defect is demonstrated within the contrast after removal of FN and ON.

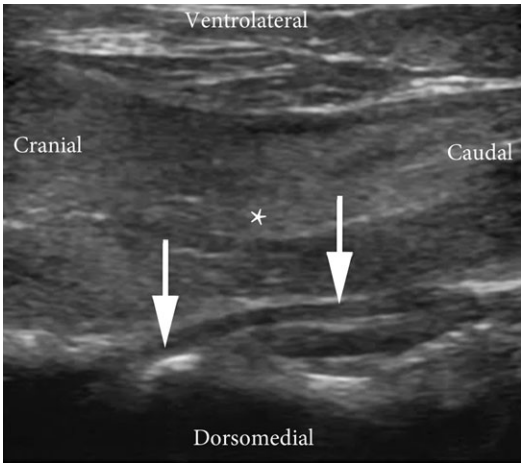

Figure 7 Ultrasound image of the femoral nerve (FN) component of the lumbar plexus (LP) in a dog using the lateral paravertebral approach to the LP at mid-L6. A longitudinal image of FN appears as a linear hypoechoic structure (white arrows). The LP, at that level, is enclosed in a fascia within the muscle bellies of the iliopsoas muscle (*).

and the contrast in 36 of 38 attempts (94%). The lateral paravertebral approach (Fig. 1) allowed imaging of the LP nerves in a longitudinal plane (Fig. 7). When utilizing the dorsal pre-iliac approach

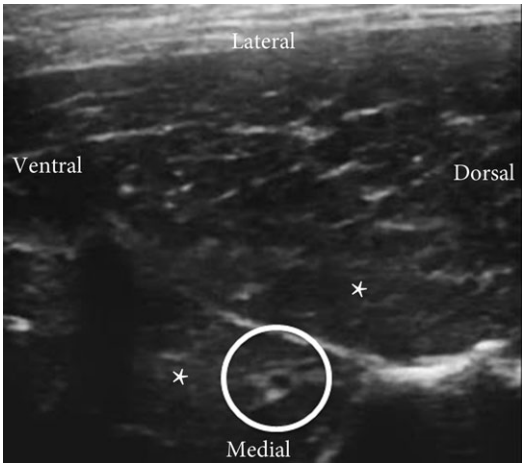

Figure 8 Ultrasound image of the femoral nerve (FN) component of the lumbar plexus (LP) in a dog using the dorsal pre-iliac approach. A transverse section of the femoral nerve is evident as a small, hypoechoic circular structure (within the white circle). The LP, at that level, is enclosed in a fascia within the muscle bellies of the iliopsoas muscle (*).

(Fig. 2), a transverse image of the LP was obtained (Fig. 8). It was noted that U/S imaging did not allow precise distinction of individual nerves leaving the LP. For this reason, the nervous structure was defined as LP rather than individual FN or ON.

There was no significant difference in distribution of contrast between the dorsal and lateral approaches (Table 1). The contrast extended from L4 to S1, travelling an average of three times the length of L6, and extending both cranial and caudal to the site of injection. The injectate formed an ovoid shape, flattened medio-laterally between the quadratus lumborum, iliopsoas and psoas minor muscles. Dorsal and ventral spread of the solution was limited, and predominantly constrained by these muscles (Fig. 5). The most caudal portion of the psoas compartment, at the level of the L6–L7 intervertebral space, consisted mainly of the iliopsoas and the psoas minor muscles, forming a clearly evident sheath where the FN and the ON were contained. More caudally, the ON stayed dorsal and medial to the sheath and remained close to the spinal column before diverging distally at the level of the body of the ilium.

Staining (≥2 cm) of the FN occurred consistently following both dorsal and lateral approaches (Table 2). The ON was stained (≥2 cm) in only nine of 38 injections (Fig. 9a & b). Distances between the edge of the contrast and the three vertebral foraminae (L5–6, L6–7 and L7–S1) were not different between the pre-iliac and the lateral paravertebral approaches at the level of L6 (Table 2). There was no evidence of abdominal or epidural injection of contrast in any dog.

A filling defect (Fig. 6b) could be identified in the area of the FN, within the mass of contrast in all but three cases, two where the FN was well stained. Length of this defect could be estimated by viewing subsequent 1.25 mm slices, and averaged 28.5 ± 13.7 mm and 30.0 ± 9.5 mm with the dorsal pre-iliac and lateral paravertebral approaches, respectively. There was no significant difference in the length of this filling defect between approaches (Table 2). No similar defect was identified in the location of the ON.

Table 1 Features of the injectate as measured following ultrasound-guided injection with subsequent CT image analysis, in 29 dogs. Bilateral plexus injections in all dogs, utilizing either a dorsal pre-iliac approach to the lumbar plexus at the 6th lumbar vertebra (dorsal approach) or a lateral paravertebral approach to the lumbar plexus at either the 6th (lateral L6) or 7th (lateral L7) lumbar vertebra. *n* = number of injections performed with each approach

	Approach to lumbar plexus			
Variable	**Dorsal (*n* = 19)**	**Lateral L6 (*n* = 19)**	**Lateral L7 (*n* = 20)**	***p* Value**
Contrast length (mm)	67 ± 20	70 ± 18	78 ± 17	0.12
Contrast length as multiple of L6	2.9 ± 0.8	2.9 ± 0.6	3.1 ± 0.8	0.69
Spread of contrast (range)	L4–S1	L5–S1	L5–S1	ND
Distance from edge of contrast to intervertebral (IV) foramen at L5 (mm)	12 ± 4	13 ± 8	ND	0.56
Distance from edge of contrast to IV foramen at L6 (mm)	12 ± 5	13 ± 3	9 ± 3*	<0.001
Distance from edge of contrast to IV foramen at L7 (mm)	23 ± 8	23 ± 5	14 ± 3*	<0.001

L, lumbar; S, sacral; NA, not available. Mean ± SD. *Significantly different from other two approaches to LP.

Table 2 Staining ≥2 cm of the femoral and obturator nerves, and nerve-induced filling defects in injectate, following ultrasound-guided injection with subsequent CT image analysis and regional dissection, in 29 dogs. Bilateral plexus injections in all dogs, utilizing either a dorsal pre-iliac approach to the lumbar plexus (LP) at the 6th lumbar vertebra (dorsal approach) or a lateral paravertebral approach to the LP at either the 6th (lateral L6) or 7th (lateral L7) lumbar vertebra. *n* = number of injections performed by each approach

	Approach to lumbar plexus			
Variable	**Dorsal (*n* = 19)**	**Lateral L6 (*n* = 19)**	**Lateral L7 (*n* = 20)**	***p* Value**
Femoral nerve stained (%)	89 (17/19)	95 (18/19)	90 (18/20)	0.6
Obturator nerve stained (%)	26 (5/19)	26 (5/19)	90 (18/20)*	<0.0001
Filling defect in contrast in region of femoral nerve (mm)	29 ± 14	30 ± 10	25 ± 12	0.39
Filling defect in contrast in region of obturator nerve (mm)	NO	NO	13 ± 9	ND

NO, not observed; ND, not done. Filling defect mean ± SD. *Significant difference from other two approaches to LP.

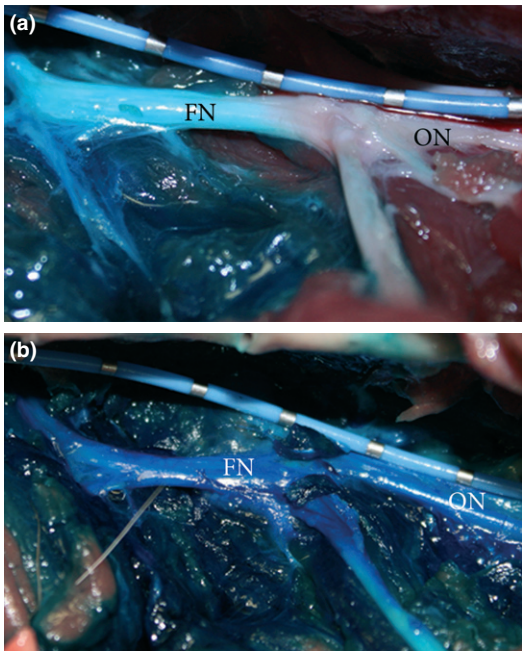

Figure 9 (a, b) Dissected femoral (FN) and obturator (ON) nerves after ultrasound-guided injection of a new methylene blue mixture. Each graduation on the marker is 1 cm, and staining over 2 cm was considered positive. In dog (a), positive staining for the FN and negative staining for the ON were observed, and in dog (b), both FN and ON demonstrated positive staining.

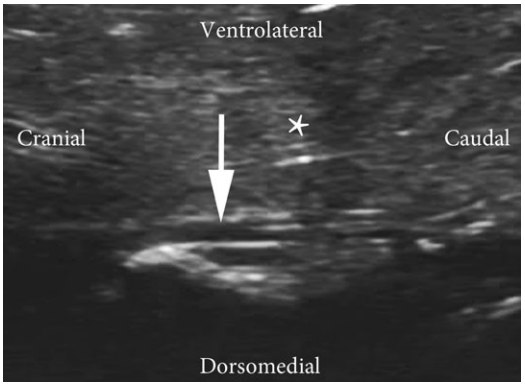

Figure 10 Ultrasound image of the femoral nerve (FN) component of the lumbar plexus (LP) in a dog using the lateral paravertebral approach to the LP at mid-L7. A longitudinal image of FN appears as a linear hypoechoic structure (white arrow). The LP, at that level, is enclosed in a fascia within the muscle bellies of the iliopsoas muscle (*).

Study 2 – evaluation of the lateral approach at L7

The lateral approach at L7 (Fig. 10) allowed consistent U/S imaging of the LP, the needle and the contrast as injected. The contrast travelled both cranially and caudally from the site of injection, extending an average of three times the length of L6 (Table 1). The injectate formed a long, ovoid shape, flattened medio-laterally, with spread of the solution constrained by the adjacent structures as previously mentioned. This injection at mid-L7 resulted in significantly closer proximity of the contrast to the L6–7 and L7–S1 foraminae (Table 1) as compared to either approach at mid-L6.

A filling defect could be identified within the mass of contrast, in the area of the FN, for all but two injections. A filling defect was also readily identified in the location of the ON for all but two injections, and this defect could be measured, averaging 13.3 ± 9.1 mm in length (Table 2). The absence of filling defect correlated with the

complete absence of staining of FN or ON. The rate of positive FN staining was not different for the three approaches at the level of L6 or L7, but the positive ON staining rate was significantly higher with injection at L7 (Table 2) compared to the injections at the level of L6. There was no evidence of abdominal or epidural injection of contrast in any dog.

Discussion

In this study all the approaches allowed easy imaging of the LP. The pilot study verified that the identified nerves corresponded to the FN and ON component of the LP. The nerves of the LP appeared as previously described, as a hypoechoic bundle surrounded by a thin hyperechoic layer (Echeverry et al. 2012b). The U/S-guided lateral paravertebral approach to the LP provided an accurate method for deposition of injected solution near the FN. Results indicated that a more caudal approach to the LP at the level of L7 was necessary to ensure that the ON was also bathed in contrast.

Anatomical studies in dogs and clinical trials in humans have demonstrated the importance of the ON in the stifle (or knee) sensory innervation. In dogs, the ON contributes to sensation through medial capsular nerve branches (O'Connor & Woodbury 1982; McNamee et al. 2002; Macalou et al. 2004; Sakura et al. 2010). At present, the most common orthopedic procedure performed at our institution is tibial plateau leveling osteotomy (TPLO), which involves a medial approach to the stifle and proximal tibia. Therefore, locoregional anesthesia should target the ON in addition to the ScN and FN for stifle surgery. This study was designed to derive an accurate means of locating the LP and subsequently blocking the FN and ON. We evaluated the FN and ON as those two nerves are the main components of the LP innervating our area of interest. The dorsal pre-iliac or lateral paravertebral, U/S guided approaches at the level of the lumbar spine allowed easy imaging and staining of the LP, with no evidence of intra-abdominal or epidural contamination based on CT scan analysis. Ultrasound guidance allowed easy, precise and rapid performance of the injection. It also enabled monitoring of the dispersion of the injectate during delivery. From a dorsal pre-iliac approach, the LP was viewed in cross-section between transverse processes. The lateral paravertebral approach to the plexus allowed longitudinal visualization of the LP as it runs below the transverse processes and lateral to the vertebral bodies, thus making the U/S target larger and the block subjectively easier to perform.

In the present study, small volumes of injectate were utilized (0.1 mL kg^{-1}). The accurate delivery and thus effective nerve staining using this small volume should translate into reduced dosage of local anesthetic solution in clinical patients, decreasing the potential for toxicity. However, a clinical study is necessary to determine optimal injectate volume and evaluate the risk for potential IV injection. These findings, specifically the extensive craniocaudal spread of the contrast, also suggest that it should be possible to utilize even smaller volumes of local anesthetic solution. Injectate volumes ranging from 0.2 to 0.6 mL kg^{-1}, have been investigated for the staining of the FN, and over this range, volume was shown not to influence distribution of injectate, or nerve staining (Echeverry et al. 2012b). Furthermore, injectate volume has been shown to be unrelated to the degree and duration of nerve block, with concentration of local anesthetic being more important (Portela et al. 2010).

The 3-D images allowed evaluation of the distribution of contrast material and provided evidence that the LP is encased between the fascia of the quadratus lumborum, psoas minor and the iliopsoas muscles with only the two latter muscles defining this compartment at the level of L6–L7. This virtual space, referred to as the psoas compartment, seems to dictate the behavior of the injectate, which has a tendency to disperse cranially and caudally between those muscle bellies. The contrast traveled 1–2 vertebral body lengths cranial and caudal to the site of injection. This finding is similar to that reported by Portela et al. (2012) when using an ultrasound-guided injection made from the lateral aspect of the lumbar musculature, cranial to the iliac crest. In addition, in the study presented here, the contrast was laterally compressed with minimal dorsoventral spread, suggesting the craniocaudal pathway (psoas compartment) was the path of least resistance. Whilst we expect the initial injectate to be similarly shaped *in vivo*, further diffusion may enhance its spread.

The point of injection seems to have major impact on the success of the technique if the ON is considered significant. The spread of contrast was comparable for all studied approaches, but the ON was only apparent within the body of the contrast, and stained effectively, following the injection at mid-L7. This injection site also correlated with the

shortest distance between the contrast and the L7–S1 foramen. The bifurcation of the ON from the plexus was repeatedly seen at the level of the L6–L7 interspace in all dissections. Whilst it was common to visualize the ON adjacent to the larger FN during performance of the ultrasound-guided injections, the ON was not stained by most of those injections. *In vivo*, diffusion may assist delivery of local anesthetic to the ON from the mid-L6 injection site, but that remains to be determined.

To assess the accuracy of the injections, two methods were chosen. Dissection is the standard for evaluation of the spread of local anesthetic solution but causes the anatomy to be disrupted. The CT images have the advantage of showing the spread of the contrast in 3-D, and its' location compared to the bony landmarks and the nerves. The stained section of the ON and FN was measured, and a length of nerve stained ≥2 cm was considered to be positive. Convention suggests that this amount of exposure to injectate would allow a nerve to be 'well blocked' such that clinical analgesia would have resulted (Campoy et al. 2008). Mid to large sized dogs were used in this study (21–35 kg). In the majority of cases, the nerves were easily visualized. In a small number of dogs the FN was more difficult to visualize by ultrasound, possibly due to autolysis, or large body mass.

In conclusion, a L7 paravertebral U/S-guided approach to the LP was successfully derived. This approach resulted in effective staining of the FN and ON and also extensive injectate dispersion. No contrast was deposited in either the abdominal cavity or the epidural space. Future studies should aim to assess the clinical relevance of these findings.

Acknowledgement

The authors thank Dr. Loic M Déjardin for his generous support of the study.

References

Adams D (2004) Canine Anatomy: A Systematic Study (4th edn). Blackwell Publishing, Des Moines, USA. pp. 339.

Campoy L, Martin-Flores M, Looney AL et al. (2008) Distribution of a lidocaine-methylene blue solution staining in brachial plexus, lumbar plexus and sciatic nerves in the dog. Vet Anaesth Analg 35, 348–354.

Campoy L, Martin-Flores M, Ludders JW et al. (2012) Comparison of bupivacaine femoral and sciatic nerve block versus bupivacaine and morphine epidural for stifle surgery in dogs. Vet Anaesth Analg 39, 91–98.

Caniglia AM, Driessen B, Puerto DA et al. (2012) Intraoperative antinociception and postoperative analgesia following epidural anesthesia versus femoral and sciatic nerve blockade in dogs undergoing stifle joint surgery. J Am Vet Med Assoc 241, 1605–1612.

Echeverry DF, Gil F, Laredo F et al. (2010) Ultrasound-guided block of the sciatic and femoral nerves in dogs: a descriptive study. Vet J 186, 210–215.

Echeverry DF, Laredo FG, Gil F et al. (2012a) Ventral ultrasound-guided suprainguinal approach to block the femoral nerve in the dog. Vet J 192, 333–337.

Echeverry DF, Laredo FG, Gil F et al. (2012b) Ultrasound-guided 'two-in-one' femoral and obturator nerve block in the dog: an anatomical study. Vet Anaesth Analg 39, 611–617.

Enneking FK, Chan V, Greger J et al. (2005) Lower-extremity peripheral nerve blockade: essentials of our current understanding. Reg Anesth Pain Med 30, 4–35.

Evans HE, de Lahunta A (2013) Miller's Anatomy of the Dog (4th edn). Saunders Elsevier Inc., St. Louis, USA. pp. 636–639.

Fowler SJ, Symons J, Sabato S et al. (2008) Epidural analgesia compared with peripheral nerve blockade after major knee surgery: a systematic review and meta-analysis of randomized trials. Br J Anaesth 100, 154–164.

Hendrix PK, Raffe MR, Robinson EP et al. (1996) Epidural administration of bupivacaine, morphine, or their combination for postoperative analgesia in dogs. J Am Vet Med Assoc 209, 598–607.

Jeng CL, Rosenblatt MA (2011) Intraneural injections and regional anesthesia: the known and the unknown. Minerva Anestesiol 77, 54–58.

Jones RS (2001) Epidural analgesia in the dog and cat. Vet J 161, 123–131.

Macalou D, Trueck S, Meuret P et al. (2004) Postoperative analgesia after total knee replacement: the effect of an obturator nerve block added to the femoral 3-in-1 nerve block. Anesth Analg 99, 251–254.

Mahler SP (2012) Ultrasound guidance to approach the femoral nerve in the iliopsoas muscle: a preliminary study in the dog. Vet Anaesth Analg 39, 550–554.

Mahler SP, Adogwa AO (2008) Anatomical and experimental studies of brachial plexus, sciatic, and femoral nerve-location using peripheral nerve stimulation in the dog. Vet Anaesth Analg 35, 80–89.

Marhofer P, Greher M, Kapral S (2005) Ultrasound guidance in regional anaesthesia. Br J Anaesth 94, 7–17.

McNamee DA, Parks L, Milligan KR (2002) Post-operative analgesia following total knee replacement: an evaluation of the addition of an obturator nerve block to combined femoral and sciatic nerve block. Acta Anaesthesiol Scand 46, 95–99.

O'Connor BL, Woodbury P (1982) The primary articular nerves to the dog knee. J Anat 134, 563–572.

Portela DA, Otero PE, Tarragona L et al. (2010) Combined paravertebral plexus block and parasacral sciatic block in healthy dogs. Vet Anaesth Analg 37, 531–541.

Portela DA, Otero PE, Briganti A et al. (2012) Femoral nerve block: a novel psoas compartment lateral pre-iliac approach in dogs. Vet Anaesth Analg 40, 194–204.

Rasmussen LM, Lipowitz AJ, Graham LF (2006) Controlled, clinical trial assessing saphenous, tibial and common peroneal nerve blocks for the control of perioperative pain following femoro-tibial joint surgery in the nonchondrodystrophoid dog. Vet Anaesth Analg 33, 49–61.

Raymond SA, Steffensen SC, Gugino LD et al. (1989) The role of length of nerve exposed to local anesthetic and impulse blocking action. Anaesth Analg 68, 363–370.

Sakura S, Hara K, Ota J et al. (2010) Ultrasound-guided peripheral nerve blocks for anterior cruciate ligament reconstruction: effect of obturator nerve block during and after surgery. J Anesth 24, 411–417.

Vettorato E, Bradbrook C, Gurney M et al. (2012) Peripheral nerve blocks of the pelvic limb in dogs: a retrospective clinical study. Vet Comp Orthop Traumatol 25, 314–320.

Received 11 February 2014; accepted 4 June 2014.

